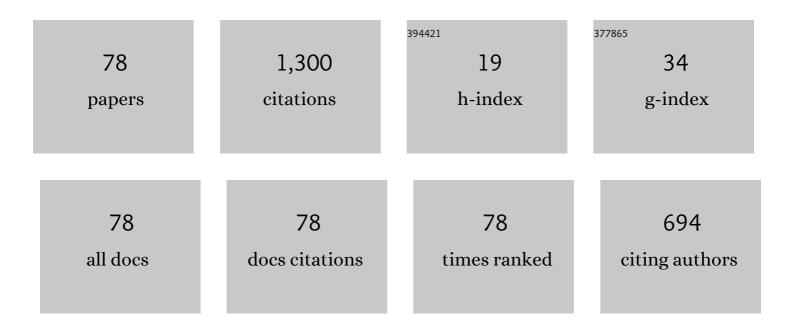


List of Publications by Year in descending order

Source: https://exaly.com/author-pdf/7161802/publications.pdf Version: 2024-02-01



LINC CAO

#	Article	IF	CITATIONS
1	The singleâ€wavelength 561 nm laser based on reflective volume Bragg grating. Microwave and Optical Technology Letters, 2023, 65, 1255-1260.	1.4	1
2	Tunable short-wave near-infrared continuous wave source based on a 532â€nm pumped singly resonant optical parametric idler oscillator. , 2022, 1, 547.		0
3	High peak power, high repetition rate electro-optically Q-switched Nd:GdTaO4 1066Ânm laser. Infrared Physics and Technology, 2022, 125, 104266.	2.9	0
4	Determination of blood species using echelle Raman spectrometer and surface enhanced Raman spectroscopy. Spectrochimica Acta - Part A: Molecular and Biomolecular Spectroscopy, 2022, 281, 121640.	3.9	3
5	Discrimination of blood species using Raman spectroscopy combined with a recurrent neural network. OSA Continuum, 2021, 4, 672.	1.8	15
6	High Dynamic Range Structured Illumination Microscope Based on Multiple Exposures. Frontiers in Physics, 2021, 9, .	2.1	3
7	<scp>Highâ€power</scp> , continuousâ€wave optical parametric oscillator based on <scp>MgO</scp> : <scp>sPPLT</scp> crystal. Microwave and Optical Technology Letters, 2021, 63, 2068-2073.	1.4	7
8	The application of bioactive pyrazolopyrimidine unit for the construction of fluorescent biomarkers. Dyes and Pigments, 2020, 173, 107878.	3.7	16
9	The identification of blood species using the correlation coefficient of sub-spectra based on Raman spectroscopy. Optik, 2020, 200, 163312.	2.9	4
10	Comparison on performances of continuous-wave and acousto-optically Q-switched Nd:GdYTaO4 lasers under 808Ânm and 879Ânm pumping. Infrared Physics and Technology, 2020, 110, 103449.	2.9	2
11	4F3/2→4I9/2 and 4F3/2→4I13/2 laser operations with a Nd:GdTaO4 crystal. Optics and Laser Technology, 2020, 131, 106444.	4.6	4
12	Harmonic mode locking underneath the Q-switched envelope in passively Q-switched mode-locked Nd:GdTaO4 1066Ânm laser. Infrared Physics and Technology, 2020, 111, 103553.	2.9	5
13	Synthesis and optical properties of bispyrazolopyridine derivatives. Dyes and Pigments, 2020, 181, 108569.	3.7	3
14	Rational design of a multifunctional molecular dye for dual-modal NIR-II/photoacoustic imaging and photothermal therapy. Chemical Science, 2019, 10, 8348-8353.	7.4	137
15	High-repetition-rate passively Q-switched Nd:GdTaO4 1066â€⁻nm laser under 879â€⁻nm pumping. Infrared Physics and Technology, 2019, 102, 103025.	2.9	6
16	Novel CW and actively Q-switched 1066 nm Nd:GdYNbO4 laser under direct pumping. Optik, 2019, 181, 398-403.	2.9	1
17	Fluorescent hydrogen sulfide probes based on azonia-cyanine dyes and their imaging applications in organelles. Analytica Chimica Acta, 2019, 1068, 60-69.	5.4	14
18	Switchable Nanochannel Biosensor for H ₂ S Detection Based on an Azide Reduction Reaction Controlled BSA Aggregation. Analytical Chemistry, 2019, 91, 6149-6154.	6.5	45

#	Article	IF	CITATIONS
19	LD pumped quasi-three-level 928â€ [–] nm laser with Nd:Gd0.69Y0.3TaO4 mixed crystal. Optics and Laser Technology, 2019, 111, 222-226.	4.6	0
20	Blood species identification based on deep learning analysis of Raman spectra. Biomedical Optics Express, 2019, 10, 6129.	2.9	24
21	Fourier based partial least squares algorithm: new insight into influence of spectral shift in "frequency domain― Optics Express, 2019, 27, 2926.	3.4	9
22	Active Q-switching operation of slab Ho:SYSO laser wing-pumped by fiber coupled laser diodes. Optics Express, 2019, 27, 11455.	3.4	20
23	926â€ ⁻ nm laser operation in Nd:GdNbO4 crystal based on 4F3/2â€ ⁻ →â€ ⁻ 4I9/2 transition. Optics and Laser Technology, 2018, 101, 515-519.	4.6	5
24	Vitamin D levels correlate with lymphocyte subsets in elderly patients with age-related diseases. Scientific Reports, 2018, 8, 7708.	3.3	19
25	Error analysis of the spectral shift for partial least squares models in Raman spectroscopy. Optics Express, 2018, 26, 8016.	3.4	13
26	Continuous-wave and pulsed 1,066-nm Nd:Gd ₀₆₉ Y ₀₃ TaO ₄ laser directly pumped by a 879-nm laser diode. Optics Express, 2018, 26, 15705.	3.4	11
27	Investigation on 13 μm laser performance with Nd:Gd069Y03TaO4 and Nd:Gd068Y03NbO4 mixed crystals. Optics Express, 2018, 26, 15785.	3.4	6
28	LD pumped 1347â€ [–] nm laser with a novel Nd:GdNbO4 crystal. Infrared Physics and Technology, 2018, 94, 32-37.	2.9	3
29	Quasi-three-level Nd:GdYNbO ₄ 927 nm laser under 879 nm laser diode pumping. Laser Physics, 2018, 28, 085803.	1.2	0
30	Dual-model analysis for improving the discrimination performance of human and nonhuman blood based on Raman spectroscopy. Biomedical Optics Express, 2018, 9, 3512.	2.9	13
31	LD pumped Nd:GdNbO4 crystal laser operating at 926 nm. , 2018, , .		0
32	Discrimination of Human and Nonhuman Blood by Raman Spectroscopy and Partial Least Squares Discriminant Analysis. Analytical Letters, 2017, 50, 379-388.	1.8	34
33	Continuous-wave yellow laser generation at 578 nm by intracavity sum-frequency mixing of thin disk Yb:YAG laser and Nd:YAG laser. Optics and Laser Technology, 2017, 92, 32-35.	4.6	11
34	Spectral Range Optimization to Enhance the Effectiveness of Phototherapy for Neonatal Hyperbilirubinemia. Journal of Applied Spectroscopy, 2017, 84, 92-102.	0.7	2
35	Continuous-wave and passively Q-switched Nd:GYTO ₄ laser. Laser Physics Letters, 2017, 14, 095802.	1.4	12
36	Diode pumped Dy:YAG yellow laser. , 2017, , .		1

#	Article	IF	CITATIONS
37	Long distance, distributed gas sensing based on micro-nano fiber evanescent wave quartz-enhanced photoacoustic spectroscopy. Applied Physics Letters, 2017, 111, .	3.3	44
38	Discrimination of human and nonhuman blood using Raman spectroscopy with self-reference algorithm. Journal of Biomedical Optics, 2017, 22, 1.	2.6	10
39	Generation of a 578-nm Yellow Laser by the Use of Sum-Frequency Mixing in a Branched Cavity. IEEE Photonics Journal, 2016, 8, 1-7.	2.0	3
40	LD pumped passively Q-switched ceramic Nd:YAG 946Ânm laser with a high peak power output. Optical and Quantum Electronics, 2016, 48, 1.	3.3	3
41	Continuous-wave and passively Q-switched 1.06μm ceramic Nd:YAG laser. Optics and Laser Technology, 2016, 81, 46-49.	4.6	17
42	Modeling and optimization of actively Q-switched Nd:GdVO4 912 nm laser. Optik, 2015, 126, 1282-1286.	2.9	1
43	Continuous-wave yellow–green laser at 056  μm based on frequency doubling of a diode-end-pumpe ceramic Nd:YAC laser. Applied Optics, 2015, 54, 5817.	d _{2.1}	16
44	All-Solid-State Continuous-wave Yellow-Green Ceramic Laser at 0.56 \hat{l} 4m. , 2015, , .		0
45	All-Solid-State Efficient CW Yellow Laser under Direct Diode-Pumping. , 2014, , .		0
46	High-power, high-repetition-rate actively Q-switched 916nm laser and the frequency doubled pulsed 458nm blue laser. Optics and Laser Technology, 2014, 58, 161-165.	4.6	1
47	Diode-pumped passively Q-switched 916nm laser with a Cr4+:YAG saturable absorber. Optics Communications, 2014, 313, 401-405.	2.1	1
48	High-power continuous-wave yellow–green laser at 558nm under in-band pumping. Optics Communications, 2014, 319, 110-112.	2.1	10
49	Study of the thermal effect in Nd:GdVO4 912 nm CW laser. Journal of Russian Laser Research, 2013, 34, 114-119.	0.6	3
50	Improvement of the Performance of an Acousto-Optical Q-Switched Nd:YAG 946Ânm Laser Using a Convex–Plane Cavity. Journal of Russian Laser Research, 2013, 34, 586-592.	0.6	0
51	Research on the optical system of neonatal jaundice phototherapy apparatus based on fly-eye lens. , 2013, , .		2
52	Modeling and optimization of actively Q-switched Nd-doped quasi-three-level laser. Optics Communications, 2013, 305, 276-281.	2.1	2
53	Highly efficient continuous-wave composite Nd:YAG laser at 1,112Ânm under diode pumping directly into the emitting level. Applied Physics B: Lasers and Optics, 2013, 111, 407-413.	2.2	10
54	High-efficiency Nd:LuVO ₄ quasi-three-level 916Ânm laser under polarized pumping. Applied Optics, 2013, 52, 4020.	1.8	1

#	Article	IF	CITATIONS
55	All-solid-state continuous-wave yellow laser at 561Ânm under in-band pumping. Journal of the Optical Society of America B: Optical Physics, 2013, 30, 95.	2.1	26
56	Efficient continuous-wave 1112 nm Nd:YAG laser operation under direct diode pumping at 885 nm. Laser Physics Letters, 2013, 10, 015802.	1.4	12
57	Quasi-three-level neodymium vanadate laser operation under polarized diode pumping: theoretical and experimental investigation. Laser Physics, 2012, 22, 1279-1285.	1.2	2
58	Diode-pumped short pulse passively Q-switched 912 nm Nd:GdVO4/Cr:YAG laser at high repetition rate operation. Laser Physics, 2010, 20, 1275-1278.	1.2	15
59	Quasi-three-level Nd:YVO4 laser operation at 914 nm under 879 nm diode laser pumping. Laser Physics, 2010, 20, 1590-1593.	1.2	22
60	Diode-laser-pumped high efficiency continuous-wave operation at 912 nm laser in Nd:GdVO4crystal. Laser Physics Letters, 2009, 6, 34-37.	1.4	32
61	Upconversion spectra of Nd:GdVO ₄ crystal under CW 808 nm diode-laser pumping. Laser Physics Letters, 2009, 6, 125-128.	1.4	28
62	Effects of energy-transfer up-conversion and excited-state absorption in quasi-three-level Nd:GdVO4 lasers. Journal of Russian Laser Research, 2009, 30, 376-383.	0.6	7
63	Improvement of diode-end-pumped 912 nm Nd:GdVO4 laser performance based on microchannel heat sink. Journal of Russian Laser Research, 2009, 30, 327-337.	0.6	9
64	456-nm deep-blue laser generation by intracavity frequency doubling of Nd:GdVO4 under 879-nm diode pumping. Laser Physics, 2009, 19, 111-114.	1.2	106
65	8.9-W continuous-wave, diode-end-pumped all-solid-state Nd:YVO4 laser operating at 914 nm. Laser Physics, 2009, 19, 389-391.	1.2	25
66	The influence of energy transfer upconversion on thermal loading in end-pumped Nd:GdVO4 laser. Laser Physics, 2009, 19, 1969-1973.	1.2	8
67	120-W continuous-wave diode-end-pumped Nd:GdVO_4 laser with high brightness operating at 912-nm. Optics Express, 2009, 17, 3574.	3.4	69
68	Comparison on performance of acousto-optically Q-switched Nd:GdVO_4 and Nd:YVO_4 lasers at high repetition rates under direct diode pumping of the emitting level. Optics Express, 2009, 17, 9468.	3.4	18
69	Laser operation at high repetition rate of 100ÂkHz in Nd:GdVO4 under 879Ânm diode-laser pumping. Applied Physics B: Lasers and Optics, 2008, 92, 199-202.	2.2	15
70	Laser operation of LD end-pumped grown-together Nd:YVO ₄ /YVO ₄ composite crystal. Laser Physics Letters, 2008, 5, 429-432.	1.4	39
71	Diode-end-pumped acousto-optically Q-switched 914 nm laser and the pulsed blue light generation by intracavity frequency doubling. Laser Physics Letters, 2008, 5, 433-436.	1.4	54
72	Pulsed 456 nm deepâ€blue light generation by acoustooptical Qâ€switching and intracavity frequency doubling of Nd:GdVO ₄ . Laser Physics Letters, 2008, 5, 577-581.	1.4	84

#	Article	IF	CITATIONS
73	Efficient generation of 914 nm laser with high beam quality in Nd:YVO4crystal pumped byï€-polarized 808 nm diode-laser. Laser Physics Letters, 2008, 5, 655-658.	1.4	29
74	Quasi-three-level Nd:GdVO ₄ laser under diode pumping directly into the emitting level. Laser Physics Letters, 2008, 5, 797-799.	1.4	33
75	Room temperature efficient continuous wave and Q-switched Ho:YAG laser double-pass pumped by a diode-pumped Tm:YLF laser. Laser Physics Letters, 2008, 5, 800-803.	1.4	56
76	Improvement in the laser performances of an A-O Q-switched Nd:GdVO4 laser by direct-diode pumping into the emitting level. Laser Physics, 2008, 18, 831-834.	1.2	10
77	Improved performance of acoustooptically Q-switched Nd:GdVO4 laser by using the planoconvex cavity. Laser Physics, 2008, 18, 1505-1507.	1.2	22
78	High Power Continuous-Wave and Acousto-Optic Q-Switched Nd:GdVO 4 Laser Operated at 912 nm. Chinese Physics Letters, 2008, 25, 119-121.	3.3	6